Effects of Mixing Localisation in LES-MMC Simulations of a Lifted Hydrogen Flame

B. Sundaram[1], M.J. Cleary[2] and A.Y. Klimenko[1]

[1]School of Mechanical and Mining Engineering
University of Queensland, St Lucia, Queensland 4072, Australia

[2]School of Aerospace, Mechanical and Mechatronic Engineering
University of Sydney, Sydney, New South Wales 2006, Australia

Abstract

This work presents sparse-Lagrangian simulations of a lifted hydrogen flame in a vitiated coflow of combustion products. An Eulerian Large Eddy Simulation generates turbulent flow field data including filtered velocity, density and a reference mixture fraction. A sparse ensemble of notional Lagrangian particles is then used to solve the Filtered Density Function for the subgrid reactive scalar quantities. A Generalised Multiple Mapping Conditioning (MMC) micro-mixing model enforces local mixing in extended space which comprises of physical space and the LES simulated reference mixture fraction. Predictions of lift-off, stabilisation and turbulent composition are obtained with as few as 23,000 Lagrangian particles while 1.9 million grid cells are used for the Eulerian LES. Lift-off height predictions are sensitive to the coflow temperature and the degree of mixing localisation. Excessive localisation in mixture fraction space or high coflow temperatures results in flame attachment while less localisation or low temperatures causes flame extinction.

Introduction

Combustion modelling involves non-linear multi-scale interactions between turbulent fluctuations and chemistry. These interactions are the subject of intensive research collaborations [9,1], with focus being directed towards Probability Density Function (PDF) models in a Large Eddy Simulation (LES) context. An advantage of PDF methods [22] is that non-linear chemical reaction rates are not averaged and thus they appear in closed form. However, the equations contain unclosed conditional scalar dissipation terms which require micro-mixing models, all of which have advantages and disadvantages. Mixing models such as Curls [6], modified Curls [14], Interaction by Exchange with the Mean (IEM) [8], Euclidean Minimum Spanning Trees (EMST) [24] which require a large number of Lagrangian particles per LES cell to resolve subgrid scale quantities are usually intensive and incur a high computational cost.

The focus of this work is on the performance of Multiple Mapping Conditioning (MMC) – a model framework [5] which combines the advantages of the PDF and Conditional Moment Closure (CMC) [17] methods. The possibility of reducing the number of particles by two to three orders of magnitude while obtaining good results by conditioning mixing on a reference variable has been demonstrated in Refs. [11,10]. In these works, localisation in mixture fraction space has been prioritised at the expense of localisation in physical space. This corresponds to the physics of non-premixed turbulent flames.

To examine the universality and understand the limitations of MMC, simulations are conducted on a lifted hydrogen flame [2]. The Cabra H_2/N_2 lifted flame is a case where lift-off and stabilisation are controlled by convective terms in addition to the details of mixing and is thus less sensitive to localisation of mixing in mixture fraction space. The lift-off height is known to increase with decreasing coflow temperature and increasing jet velocity, although it is far more sensitive to the former than the latter [3]. Additional parametric studies on the effects of coflow temperature have been conducted by Gordon et. al. [13] and Wu [25]. Both sets of experiments obtain similar trends but there is little accuracy across datasets.

PDF modelling of the Cabra H_2/N_2 lifted flame is reported in Cao et al. [3] who demonstrate the dominance of chemical kinetics on model predictions. They also show that model predictions of lift-off height can match the experimental data when the coflow temperature is artificially reduced relative to its experimental setting. Based on the observed correlation between fluctuations of reacting species and fluctuations of the mixture fraction, CMC models the chemical reaction rates by conditionally averaging them on the mixture fraction while conditional fluctuations are neglected. Relative to PDF modelling the computational cost of CMC is low. Patwardhan et al. [21] have conducted CMC modelling of the Cabra flame in the Reynolds Averaged Navier Stokes (RANS) context. Lift-off height predictions at high coflow temperatures are quite good although there is less success for co-flow temperatures below 1020 K. Navarro-Martinez and co-workers have published extensively on CMC of lifted hydrogen and methane flames using LES for the mixing field and CMC for the subgrid fluctuations of the reactive scalars [20]. Results are in good agreement with experimental data when coflow temperatures are artificially lowered. More recently, a deterministic version of MMC has reproduced the main turbulent mixing characteristics of the flame and lift-off, although downstream predictions require improvement [7].

Here, MMC is a PDF/FDF method that treats chemical reaction rates exactly without averaging. It is also draws on concepts from the CMC method as turbulent compositions are kept close to their conditional average values (although conditional fluctuations are still present). This is achieved by localising the mixing operation in the LES simulated mixture fraction space (called the reference mixture fraction).

Methodology

LES

LES equations are solved in the code, Flowsi [15]. A staggered, cylindrical Eulerian grid is applied to the domain and filtered velocities and reference mixture fractions are obtained. The dynamic Smagorinsky turbulent viscosity model [23,12] is used for the subgrid scale stresses.

FDF-MMC

The FDF is solved on an ensemble of Pope particles obeying the following stochastic equations:

$$dx_j^* = \left(\tilde{u}_j + \frac{1}{\bar{\rho}}\nabla\bar{\rho}(D + D_t)\right)dt + \sqrt{2(D + D_t)}dw_j \quad (1)$$

$$d\phi_\alpha^* = \left(W_\alpha(\phi^*) + S(\phi_\alpha^*)\right)dt \quad (2)$$

Particles advect and diffuse physically according to (1) and change properties such as mass fractions and enthalpy due to reactions and subgrid conditional scalar dissipation (mixing) according to (2). The mixing operation, S, is modeled discretely by a particle pair interaction model similar to Curl's model [6]. The timescale of mixing is linked to the ratio of scalar subgrid variance and scalar dissipation and for sparse simulations it is further scaled to account for the distance between mixing particles being greater than the LES filter length. The timescale of mixing between two particles (p and q) is given by

$$\tau_L = \frac{3\left(d_f^{p,q}\right)^2}{\Delta_E^2 \nabla\tilde{f} \cdot \nabla\tilde{f}}\frac{C_f\Delta_E^2}{2(D + D_t)} \quad (3)$$

where $d_{()}^{p,q} = |(.)^p - (.)^q|$, Δ_E is the LES filter width and $C_f = 0.1$.

MMC enforces mixing between particle pairs which are close in an extended space comprising of the reference mixture fraction and physical location. For the non-premixed flame studied here we choose a reference space given by the filtered mixture fraction, $\tilde{f}$, obtained from the Eulerian LES. Particle mixing pairs are selected by a minimisation of the normalized distance squared:

$$\hat{d}_{(p,q)}^2 = \left[\sum_{j=1}^{3}\left(\frac{d_{(x_j)}^{p,q}}{r_m}\right)^2 + \left(\frac{d_{(f^*)}^{p,q}}{f_m}\right)^2\right] \quad (4)$$

r_m and f_m are characteristic physical and reference scales, respectively.

Gradient-fractal model and localisation

The gradient-fractal model [4] is used to control the relative 'weighting' assigned to physical and reference mixture fraction scales. Inter-particle distances are explicitly linked with the number of particles through fractal analysis of isoscalar contours. Assuming that each particle pair is located within an iso-sliver of mixture fraction, thickness of each sliver can be estimated through the gradient. Slivers have fractal properties and the volume of a mixing particle pair can therefore be estimated. Based on the particle density, the volume of an individual particle in the domain can also be estimated. These volumes are then equated to form the following relationship:

$$r_m = C_m\left(\frac{d\tilde{f}}{dn}\frac{\Delta_L^3}{\Delta_E^{2-D_f}}\frac{1}{f_m}\right)^{1/D_f} \quad (5)$$

f_m is selected as a global parameter which determines r_m. f_m is the main tuneable parameter in these simulations and controls extent of localisation in the extended space. As its value decreases, mixing becomes more local in mixture fraction space.

Numerical Simulations

The central nozzle of the burner has a diameter of 4.57 mm (d) and extends 70 mm above the perforated base plate. The jet fuel composition by volume is 25% H_2 and 75% N_2. The jet enters the domain at a temperature of 305 K and has a bulk velocity of 107 m/s. The vitiated coflow enters the domain through an annulus of 105 mm radius. The coflow is composed of combustion products from a premixed H_2 and air flame at a temperature of 1045 K and

bulk velocity of 3.5 m/s. The stoichiometric mixture fraction is 0.47. Boundary conditions are set according to these specifications [2] in the simulations.

Jet and coflow velocity profiles are obtained from measured data [16]. The computational domain consists of a cylindrical LES grid with an axial length of 298.5 mm or 65d and a radial extent of 228.5 mm or 50d. The grid contains 1026 axial, 55 radial and 32 azimuthal finite volume cells. The smallest cells along the axis are 1mm by 0.3 mm by $\pi/32$ radians. For the stochastic composition field, approximately 23,000 Pope particles are used across the flow domain. This is equivalent to one particle per eight LES cells.

Reaction source terms are evaluated from the chemical kinetics scheme of Mueller [19] containing 9 species and 21 reactions. Simulations have been performed for artificially altered coflow temperatures of 1015, 1020, 1030, 1045, 1060 and 1080 K and localisation f_m was varied.

Results

Experimental data on species, temperature and mixture fraction is produced in both radial (z) and (x) axial directions. Experimental scatter data on species and temperature is available for x/d of 8, 9, 10, 11, 14 and 26. In the Cabra data, there is an experimental uncertainty in temperature data of 3%.

The results shown in this section correspond to a fixed coflow temperature of 1045 K (Cabra conditions). Based on previous work on the Sandia flame series, where localisation of particle pairs is 0.03 [10] f_m values ranging from 0.01 to 0.05 are tested here. Results for f_m of 0.03, 0.04 and 0.05 are shown. Each localisation value produced significantly different results.

Mixture fraction

Figure 1 displays the axial mixture fraction profile for the selected coflow temperature and localisation values. The degree of localisation controls the decay rate of mixture fraction. An f_m value equal to or greater than 0.04 produces a reasonable match with experimental data. If mixing is excessively localised, diffusivity is limited and experimental mixture fraction profiles cannot be reproduced.
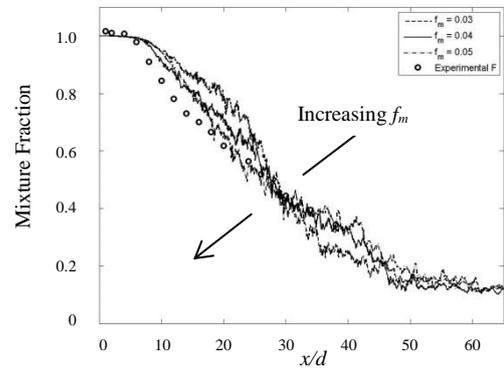
Figure 1. Axial profile of mean mixture fraction for f_m = 0.03, 0.04 and 0.05 at T_c = 1045 K.

Particle pair separation

The impact of selecting a single localisation parameter across the whole domain on the distance between particle pairs is shown in figure 2. Figure 2 indicates that lower localisation increases separation between mixing pairs in mixture fraction space. Pairs are far apart near the nozzle up to x/d = 5 and separation length steadily decreases until the end of the domain. Separation distance is not constant as the grid does not expand with jet diameter.
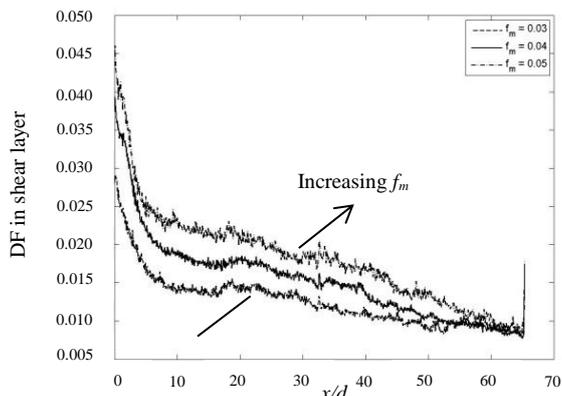
Figure 2. Axial profile of average particle pair separation in mixture fraction space for f_m = 0.03, 0.04 and 0.05 at T_c = 1045 K.

Temperature

Figure 3 shows mean axial temperature profiles. All selected localisation values produce a lower mean temperature relative to experimental results. In particular, f_m of 0.05 significantly underestimates temperature.
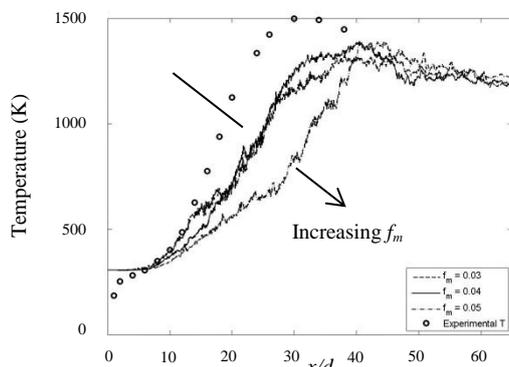
Figure 3. Axial profile of average temperature (K) for f_m = 0.03, 0.04 and 0.05 at T_c = 1045 K.

Figure 4 shows experimental and predicted scatter plots of temperature versus mixture fraction at various locations for the selected localisation values. Due to the sensitivity of lift-off height to experimental and simulation parameters, data in Figure 4 cannot be compared directly. Trends are compared instead.

x/d	Experiment	f_m = 0.03	f_m = 0.04	f_m = 0.05
1	-			
10				
14				
26				
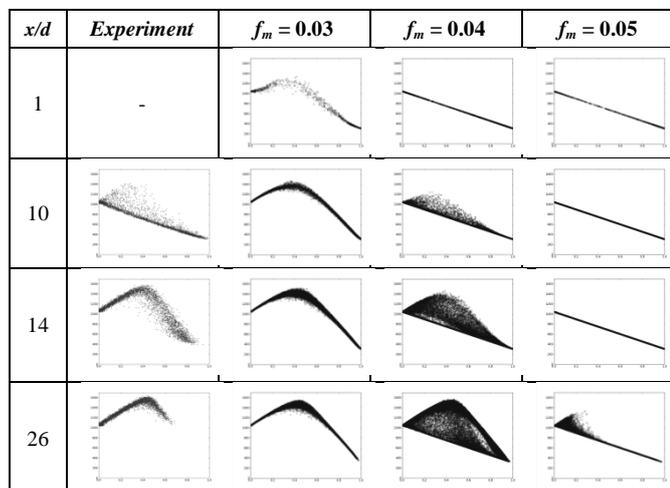
Figure 4. Scatter plots of temperature (K) at several axial locations for f_m = 0.03, 0.04 and 0.05 at T_c = 1045 K. All axes are of temperature (K) versus particle mixture fraction (Z).

In the most localised case (f_m = 0.03), the flame is in equilibrium at x/d = 1, indicating that there is no lift-off. For the less localised cases, a mixing line is visible near the inlet, indicating that lift-off has occurred. The f_m = 0.04 case produces the closest trend to experimental data for the 1045 K setting of coflow temperature.

Scalars

Figure 5 shows mean the mass fraction of OH in the axial direction. Insufficient localisation (f_m = 0.05) which delayed development of the temperature also results in delayed production of OH, an indicator of reaction. As before, f_m = 0.04 is the closest result to experimental data.
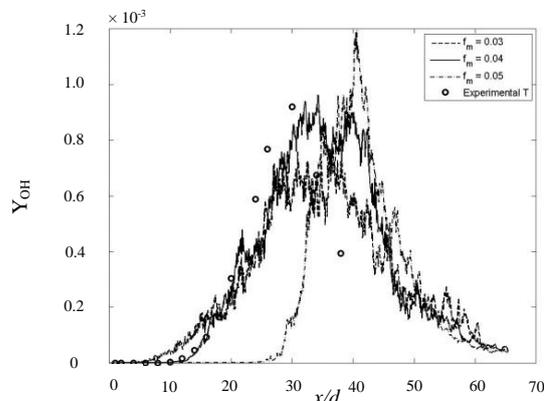
Figure 5. Axial profile of average temperature (K) for f_m = 0.03, 0.04 and 0.05 at T_c = 1045 K.

In Figure 6 a fully attached flame is seen where f_m = 0.03, with reactions beginning near the nozzle. The f_m = 0.04 and 0.05 cases indicate a delay in ignition, although the 0.05 case is approaching extinction.

x/d	Experiment	f_m = 0.03	f_m = 0.04	f_m = 0.05
1	-			
10				
14				
26				
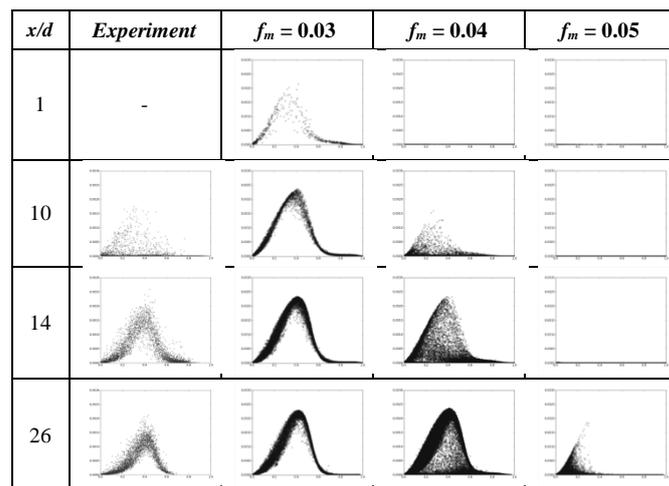
Figure 6. Scatter plots of Y_{OH} at several axial locations for f_m = 0.03, 0.04 and 0.05 at T_c = 1045 K. All axes are of Y_{OH} versus particle mixture fraction (Z) which ranges from zero to unity.

Lift-off heights

The criteria for liftoff is defined where the mean mass fraction of OH reaches at value of 2×10-4 at any radius [3].

Excessive localisation in mixture fraction space i.e. $f_m \leq 0.03$ or high coflow temperatures i.e. $T_c \geq 1060$ K result in a fully attached flame. Low localisation i.e. $f_m > 0.05$ and low coflow temperatures cause the flame to approach extinction, as indicated in Figure 7.
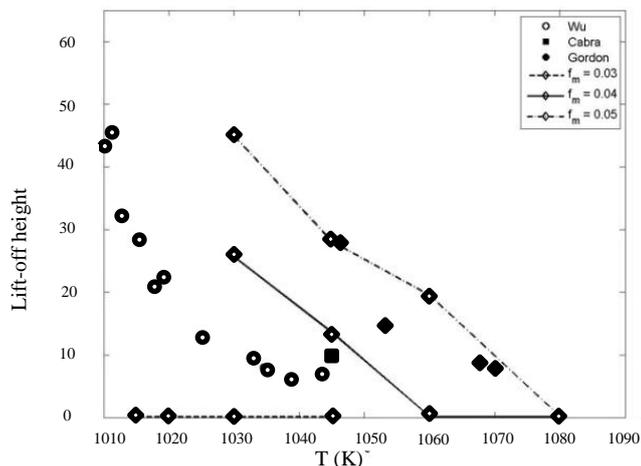
Figure 7. Lift-off height versus coflow temperature (K) for f_m = 0.03, 0.04 and 0.05.

Conclusions

The LES-FDF method with sparse-Lagrangian particles mixing based on MMC can capture lift-off and stabilisation of the Cabra hydrogen lifted flame. The trends obtained for lift-off height over a range of coflow temperatures are consistent with experiments and simulations performed by others. Both localisation and coflow temperature are highly influential on flame attachment, lift-off and stabilisation, and extinction. For low f_m values which denote a high level of localisation in mixture fraction space, the flame is not lifted. A higher f_m reduces localisation and at low coflow temperatures, results approach global extinction. Proposed improvements to the current implementation for improved downstream predictions are a flexible localisation algorithm for particle pair selection or adjustment of particle distribution according to jet development. Secondary improvements include an axially expanding grid or adjustment of the mixing timescale. The decoupling of physical and The selection of reference variables is currently being examined Currently, a range of suitable f_m values ($0.03 < f_m < 0.04$) for the tested temperatures has been identified.

Acknowledgements

References

[1] Bilger, R.W., Pope, S.B., Bray, K.N.C. & Driscoll, J.F., Paradigms in turbulent combustion research, *Proc. Combust. Inst.,* **30**, 2005, 21-42.

[2] Cabra, R., Myhrvold, T., Chen, J.Y., Dibble, R.W., Karpetis, A.N. & Barlow, R.S., Simultaneous laser Raman-Rayleigh-LIF measurements and numerical modelling results of a lifted turbulent H_2/N_2 jet flame in a vitiated coflow, *Proc. Combust. Inst.*, **29**, 2002, 1881-1888.

[3] Cao, R.R., Pope, S.B. & Masri, A.R., Turbulent lifted flames in a vitiated coflow investigated using joint PDF calculations, *Combust. Flame*, **142**, 2005, 438-453.

[4] Cleary, M.J. & Klimenko, A.Y., A detailed quantitative analysis of sparse-Lagrangian filtered density function simulations in constant and variable density reacting jet flows, *Phys. Fluids*, **23**, 2011, 115102.

[5] Cleary, M.J. & Klimenko, A.Y., In T. Echekki, E. Mastorakos (editors) *Turbulent Combustion Modelling: Advances, New Trends and Perspectives*, New York, Springer, 2011.

[6] Curl, R.L., Dispersed phase mixing: I. Theory and effects of simple reactors, *AIChE J.*, **9**, 1963, 175-181.

[7] Devaud, C.B., Stankovic, I. & Merci, B., Deterministic Multiple Mapping Conditioning (MMC) applied to a turbulent flame in a Large Eddy Simulation (LES), *Proc. Combust. Inst.*, **34**, 2012, http://dx.doi.org/10.1016/j.proci.2012.06.076.

[8] Dopazo, C. & OBrien, E.E., An approach to the autoignition of a turbulent mixture, *Acta Astronaut*, **1**, 1974, 1239-1266.

[9] Dreizler, A. & Kempf, A., Eleventh International Workshop on Measurement and Computation of Turbulent (Non) Premixed Flames, Darmstadt, 2012.

[10] Ge, Y., Cleary, M.J. & Klimenko, A.Y., A comparative study of Sandia flame series (D-F) using sparse-Lagrangian MMC modelling, *Proc. Combust. Inst.*, **34**, 2012, http://dx.doi.org/10.1016/j.proci.2012.06.059.

[11] Ge, Y., Cleary, M.J. & Klimenko, A.Y., Sparse-Lagrangian FDF simulations of Sandia Flame E with density coupling, *Proc. Combust. Inst.*, **33**, 2011, 1401-1409.

[12] Germano, M., Piomelli, U., Moin, P. & Cabot, W., A dynamic subgrid-scale eddy viscosity model, *Phys. Fluids*, **3**, 1991, 1760-1765.

[13] Gordon, R.L., Starner, S.H., Masri, A.R. & Bilger, R.W., Further characterisation of lifted hydrogen and methane flames issuing into a vitiated coflow, *Proc. Fifth Asia-Pac. Conf. Combust*, 2005.

[14] Janicka, J., Kolbe, W. & Kollmann, W., Closure of the transport equation for the probability density function of turbulent scalar field, *J. Non-Equil. Thermodyn.,* **4**, 1979, 47-66.

[15] Kempf, A., Large-Eddy Simulation of Non-Premixed Turbulent Flames, PhD Thesis, VDI Verlag GmbH, Darmstadt, 2003.

[16] Kent, J., B.E. Thesis, University of Sydney, 2003.

[17] Klimenko, A.Y. & R.W. Bilger, Conditional moment closure for turbulent combustion, *Prog. Energy Combust. Sci.*, **25**, 1999, 595-687.

[18] Li, J., Zhao, Z., Kazakov, A. & Dryer, F,L., An updated comprehensive kinetic model of hydrogen combustion, *Fall Tech. Meeting East. States Sec. Combust. Inst.*, 1999, 113-125.

[19] Mueller, M.A., Kim, T.J., Yetter, R.A. & Dryer, F.L., Flow reactor studies and kinetic modelling of the H_2/O_2 reaction, *Int. J. Chem. Kin.*, **31**, 1999, 113-125.

[20] Navarro-Martinez, S., Kronenburg, A., Flame stabilization mechanisms in lifted flames, *Flow, Turb. Combust.*, **87**, 2011, 377-406.

[21] Parthwardhan, S.S., De, S. & Lakshmisha, K.N. & Raghunundan B.N., CMC simulations of lifted turbulent jet flame in a vitiated coflow, *Proc. Combust. Inst*. **32**, 2009, 1705-1712.

[22] Pope, S.B., PDF Methods for Turbulent Reactive Flows, *Prog. Energy Combust. Sci.*, **11**, 1985, 119-192.

[23] Smagorinsky, J. General circulation experiments with the primitive equations I: the basic experiment, *Mon. Weather Rev.*, **191**, 1963, 99-164.

[24] Subramaniam, S. & Pope, S.B., A mixing model for turbulent reactive flow base on Euclidean minimum spanning trees, *Combust. Flame*, **115**, 1998, 487-514.

[25] Wu, Z., Starner, S.H. & Bilger, R.W., Lift-off heights of turbulent H2/N2 jet flames in a vitiated co-flow, *Proc. Aust. Symp. Combust.*, 2003.